



## A NUMERICAL SOLUTION OF THE MAGNETOCONVECTION OF TWO-IMMISCIBLE FLUIDS INSIDE A PARALLEL-PLATE CHANNEL

**João A. Lima**

**Bruno N.M. Silva**

PPGEM/DEM/CT/UFRN - Av. Senador Salgado Filho, sn - Lagoa Nova, Natal - RN, Brazil, 59072-970

[jalima@ufrnet.br](mailto:jalima@ufrnet.br); [darker665@hotmail.com](mailto:darker665@hotmail.com)

**Hérico S. Paiva**

**Philippe E. Medeiros**

DEM/CT/UFRN - Av. Senador Salgado Filho, sn - Lagoa Nova, Natal - RN, Brazil, 59072-970

[herico\\_silva@hotmail.com](mailto:herico_silva@hotmail.com); [philippecnrn@hotmail.com](mailto:philippecnrn@hotmail.com)

**Abstract.** A numerical approach for analysis of the fully developed magnetohydrodynamic stratified two-fluid flow with heat transfer inside an inclined parallel-plate channel is presented. In general, two incompressible, electrical conductors, immiscible, and newtonian fluids are allowed to simultaneously flow inside the channel in the steady-state regime. In order to handle as many configuration as possible under a single formulation, the upper and lower plates can be made stationary or moving at constant velocities, and a constant magnetic field is externally applied in an inclined direction relative to flow development axis. The induced magnetic field in the flow direction is also evaluated, although its influence on flow behavior is neglected, i.e., it is considered small magnetic Reynolds number. Both plates are held at constant equal or unequal temperatures and thermophysical properties are taken as constant. In addition to Joule and viscous heating, other heat generation (source) or absorption (sink) phenomena are also allowed to occur inside the flow. The governing non-linear and coupled momentum, energy and induced magnetic field equations are solved as a system of first-order ordinary differential equations through a well-established numerical routine for solution of stiff two-point boundary value problems. Results are presented both in tabular and graphical forms for a large range of the governing parameters showing the versatility of the present approach. From the results, it was found that with suitable values of the ratio of depths, angle of inclination, viscosities, thermal and electrical conductivities, the fully developed velocity, temperature and induced magnetic fields can be radically modified.

**Keywords:** Magnetohydrodynamic (MHD), Two-fluid immiscible flow, Stratified flow, Mixed convection, Numerical solution

### 1. INTRODUCTION

In the last decades, a significant increase in the study and application of electrically conducting fluid flows under the effect of magnetic fields (MHD) in ducts and enclosures has been observed. This was mainly motivated by important industrial application in metallurgy, and more recently, in other technological uses such as MHD power generators and nuclear engineering (Davidson, 2001). Furthermore, these studies are now driven by environmental issues, inasmuch as use of natural energy resources has led to generation of pollution and climate changes.

Since the early 1960's, single-phase flow and heat transfer of electrical-conductor fluids inside channels submitted to magnetic fields have been extensively studied by many authors covering different aspects that influence the various governing mechanisms. A comprehensive review is obtained following the works of Tao (1960), Nigam and Singh (1960), Perlmutter and Siegel (1961), Roming (1961) and Alpher (1961). Later, studies were resumed taking into account more physical effects, such as variable transport properties (Klemp *et al.*, 1990; Shahai, 1990; Setayesh and Sahai, 1990; Attia and Kotb, 1996; Attia, 1999; Attia, 2006), ion slip (Attia and Aboul-Hassan, 2003), and Hall interaction (Attia, 1998; Attia and Aboul-Hassan, 2003), among others.

In turn, due to the petroleum industry interest, stratified flow of two immiscible liquids has been studied, both theoretical and experimentally. The interest in these problems stems from the possibility of reducing the power required to pump oil in a pipeline by suitable addition of water, for example. In addition, when considering liquid metals as heat transfer agents or as working fluids, it was found that the power requirement could be further reduced. Shail (1973), by studying the problem of fully-developed two-fluid flow in a horizontal channel and considering a layer of non-conducting fluid overlying a conducting one, predicted the increase in the flow rate for suitable values of some governing parameters. Later, Lohrasbi and Sahai (1988) extended the problem by including heat transfer in the analysis. Malashetty and Leela (1991) and Malashetty and Leela (1992) assumed the fluid in both regions to be electrically conducting and studied the heat and fluid flow for short and open circuit cases, respectively.

All these studies had limited their attention to the MHD two-fluid flow and heat transfer in horizontal channels. On the other hand, since some applications are closer to inclined geometries, several works have been reported on literature considering this possibility. Motivated by the works of Shail (1973) and Lohrasbi and Sahai (1988), in which only one fluid is electrical conductor, Malashetty and Umavathi (1997) employed the regular perturbation method to find

approximated solutions for the mixed magnetoconvection of the two-immiscible fluids in an inclined channel. To apply the method, they studied situations where the product of Prandtl and Eckert numbers (the perturbation parameter) was very small. Later on, Malashetty *et al.* (2001a) and Malashetty *et al.* (2001b) solved the same problem, but considered both fluids electrical conductors, because in the high temperature environment of a MHD generator both fluid are expected to be electrically conducting.

The limiting case of vertical channels was further analyzed by Umavathi *et al.* (2005), who studied the mixed convection of two immiscible, electrically conducting fluids in the presence of an applied electric field parallel to gravity and a magnetic field normal to gravity. In addition to Joule and viscous dissipation, they also took into account heat generation or heat absorption in both flow regions. Later, Malashetty *et al.* (2006) studied the same configuration, but considering only one region filled with an electrically conducting fluid.

Influence of moving plates and inclined magnetic fields on flow and heat transfer characteristics has been recently studied for the forced two-phase immiscible flow in inclined channels by Umavathi *et al.* (2010) and Zivojin *et al.* (2010). Umavathi *et al.* (2010), by considering only an electrically conducting fluid and that the upper plate moves with constant velocity, studied the mixed convection employing the approximate regular perturbation method. Zivojin *et al.* (2010) extended this problem by considering both fluids were electrically conductors and both plates moves with constant but different velocities. More recently, Nikodijevic *et al.* (2011) published a similar work for horizontal channels, but fixed the lower plate and considered only one fluid as electrical conductor. Analytical solutions were obtained for velocity, temperature and induced magnetic fields for those two last works.

The main goal of this short introduction was to show how important features on magnetoconvection of two-immiscible fluid inside channels have been gradually incorporated along the years. Where possible, it was showed that some analytical solutions were obtained; however, when taking into account more physical effects, equations became strongly coupled and non-linear so that only approximate analytical results has been presented by some authors, by considering the limiting case of some dimensionless parameters. Therefore, the aim of the present work is to illustrate an efficient numerical approach for solution of the fully-developed magnetohydrodynamic two-fluid immiscible flow with heat transfer in inclined channels that can take into account several other physical aspects in a single methodology (one or two electrically conducting fluids; horizontal, vertical, and inclined channels; flow in porous layers; heat generation or absorption; forced, free or mixed convection, among others effects).

## 2. MATHEMATICAL FORMULATION

The physical configuration of the problem is sketched on Fig. 1. It consists of two inclined parallel plates that are infinitely extended in  $X$  and  $Z$  directions, and inclined by an angle  $\phi$  to the horizontal. The regions delimited by  $0 \leq y \leq h_1$  and  $-h_2 \leq y \leq 0$  are named Regions I and II, respectively. These plates are held at constant temperatures,  $T_{w1} \geq T_{w2}$ . The upper and lower plates are allowed to move with constant velocities  $U_{w1}$  e  $U_{w2}$ , respectively. Fluids flowing in Regions I and II are also driven by a common constant pressure gradient and have different densities  $\rho_i$ , viscosities  $\mu_i$ , electrical conductivities  $\sigma_i$ , magnetic permeability  $\mu_{ei}$ , and thermal conductivities  $k_i$ .

A constant magnetic field of strength  $B_0$  is applied in a direction that forms an angle  $\beta$  to the  $Y$  axis. Due to the fluid motion, an induced magnetic field of strength  $B_x$  along the flow direction is generated. In this case, the total magnetic field can be decomposed into the applied and the induced parts,  $\vec{B} = \vec{B}_x + \vec{B}_0 = (B_x(y) + B_0\sqrt{1-\lambda^2})\vec{i} + B_0\lambda\vec{j}$ , where,  $\lambda = \cos \beta$ . Despite this induced magnetic field be small,  $\vec{B}_x \ll \vec{B}_0$ , not influencing the flow field (the small magnetic Reynolds number hypothesis), it is here evaluated to show its linkage with the flow field. Hall and ion-slip effects, which introduce additional spatial complexities to the problem, are neglected.

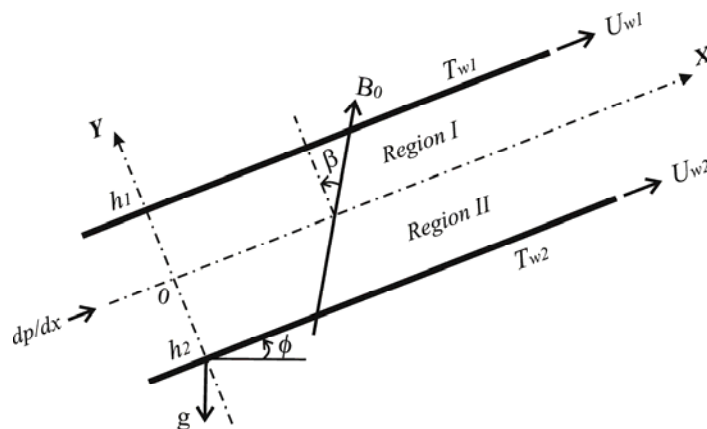


Figure 1. Physical configuration

Additionally, flow and heat transfer of viscous fluids through permeable-walled passages is very important in many branches of engineering, *e.g.*, permeable-walled ducts in heat exchangers, transpiration cooling of gas turbine blades, porous-walled reactors (Malashetty *et al.*, 2004). Therefore, in the present formulation it is allowed that one, or both regions, be homogeneous and isotropic porous media, with permeability  $k_{pi}$ , represented by a Darcian dissipation model. Fluid within the porous medium saturates the solid matrix and both are in local thermodynamic equilibrium. All properties are constant, except for the buoyancy term, since mixed convection is also analyzed by taking the Overbeck-Boussinesq approximation. In addition to viscous and Joule heating, other effects of temperature-dependent heat generation or absorption (due to exothermic and endothermic reactions, for example) are explicitly taken into account through coefficients  $q_i$ .

Under these suppositions, the dimensionless governing equations for the laminar, fully developed flow and heat transfer are written for phase  $i$  as:

$$-mh^2P + \frac{d^2u_i}{dy^2} + r b h^2 m \frac{Gr}{Re} \theta_i \sin \phi - Ha_i^2 \lambda (E_z + u_i \lambda) - \varepsilon_i^2 u_i = 0 \quad (1)$$

$$\frac{d^2\theta_i}{dy^2} + Ec Pr \frac{k_c}{m} \left[ \left( \frac{du_i}{dy} \right)^2 + Ha_i^2 (Ez + u_i \lambda)^2 + \varepsilon_i^2 u_i^2 \right] + Q_i \theta_i = 0 \quad (2)$$

$$\frac{d^2B_{xi}}{dy^2} + \lambda s h m_e Rm \frac{du_i}{dy} = 0 \quad (3)$$

Subjected to the following boundary and interface conditions:

$$\left. \begin{array}{l} u_1(0) = u_2(0) \\ \frac{du_1}{dy} \Big|_{y=0} = \frac{1}{mh} \frac{du_2}{dy} \Big|_{y=0} \\ \theta_1(0) = \theta_2(0) \\ \frac{d\theta_1}{dy} \Big|_{y=0} = \frac{1}{k_c h} \frac{d\theta_2}{dy} \Big|_{y=0} \\ B_{x1}(0) = B_{x2}(0) \\ \frac{dB_{x1}}{dy} \Big|_{y=0} = \frac{1}{sh m_e} \frac{dB_{x2}}{dy} \Big|_{y=0} \end{array} \right\}, y=0; \quad \left. \begin{array}{l} u_2(-1) = u_{w2} \\ \theta_2(-1) = 0 \\ B_{x2}(-1) = 0 \end{array} \right\}, y=-1 \quad (4.a-1)$$

$$\left. \begin{array}{l} u_1(1) = u_{w1} \\ \theta_1(1) = \theta_w \equiv \begin{cases} 1, & T_{w1} \neq T_{w2} \\ 0, & T_{w1} = T_{w2} \end{cases}, y=1; \\ B_{x1}(1) = 0 \end{array} \right\}$$

Equations (4.a) and (4.j) are the wall non-slip condition, Eqs. (4.b) and (4.k) are the isothermal conditions at the upper and lower plates, respectively, Eqs. (4.d-i) indicate the continuity of flow, heat transfer and magnetic fields at the interface (equal velocities, temperatures, magnetic field, interfacial flow and magnetic tensions, and heat fluxes). Equations (4.c) and (4.h) are the prescribed magnetic field on each plate.

To make equations non-dimensional, the dimensionless groups described below were used.  $Re$ ,  $Pr$ ,  $Gr$ ,  $Ec$ ,  $Ha$  and  $Rm$  are the dimensionless Reynolds, Prandtl, Grashof, Eckert, Hartmann and magnetic Reynolds numbers, respectively. Asterisks were dropped for simplicity and, for the Region I, coefficients  $b$ ,  $m$ ,  $r$ ,  $h$ ,  $k_c$ ,  $k_p$ ,  $s$  and  $m_e$  are made unitary.

$$\begin{aligned} u_i^* &= \frac{u_i}{u_1}; & y_i^* &= \frac{y_i}{h_i}; & \theta_i &= \frac{T_i - T_{w2}}{T_{w1} - T_{w2}}; & m &= \frac{\mu_1}{\mu_2}; & k_c &= \frac{k_1}{k_2}; & k_p &= \frac{k_{p1}}{k_{p2}}; & h &= \frac{h_2}{h_1}; \\ r &= \frac{\rho_2}{\rho_1}; & b &= \frac{\beta_2}{\beta_1}; & s &= \frac{\sigma_2}{\sigma_1}; & m_e &= \frac{\mu_{e2}}{\mu_{e1}}; & Re &= \frac{\bar{u}_1 h_1}{\nu_1}; & Pr &= \frac{\mu_1 c_{p1}}{k_1}; & \varepsilon_i &= \frac{h_i}{\sqrt{k_{pi}}}; \\ P &= \frac{h_1^2}{\mu_1 u_1} \frac{\partial p}{\partial x}; & Q_i &= q_i \frac{h_i^2}{k_i}; & Gr &= \frac{g \beta_1 h_1^3 \Delta T}{\nu_1^2}; & Ec &= \frac{\bar{u}_1^2}{c_p (T_{w1} - T_{w2})}; & Ha_i &= B_0 h_i \sqrt{\frac{\sigma_i}{\mu_i}}; \\ Gr &= \frac{g \beta_1 h_1^3 \Delta T}{\nu_1^2}; & Ec &= \frac{\bar{u}_1^2}{c_p (T_{w1} - T_{w2})}; & B_{xi}^* &= \frac{B_{xi}}{B_0}; & E_z^* &= \frac{E_z}{B_0 u_1}; & Rm_1 &= \bar{u}_1 h_1 \sigma_1 \mu_{e1} \end{aligned} \quad (5)$$

Now, in order to map all fluid regions in a single numerical domain  $[0,1]$ , the procedure employed by Van Gorder *et al.* (2012) to map Region II from  $[-1,0]$  to  $[0,1]$  was adopted. To do this, functions  $\hat{u}_2(y) = u_2(-y)$ ,  $\hat{\theta}_2(y) = \theta_2(-y)$  and  $\hat{B}_{x2}(y) = B_{x2}(-y)$  are defined, so that Eqs.(1-4) for this new domain are rewritten as:

$$-P + \frac{d^2 u_1}{dy^2} + \frac{Gr}{Re} \theta_1 \sin \phi - Ha_1^2 \lambda (E_z + u_1 \lambda) - \varepsilon_1^2 u_1 = 0 \quad (6)$$

$$\frac{d^2 \theta_1}{dy^2} + Ec Pr \left[ \left( \frac{du_1}{dy} \right)^2 + Ha_1^2 (E_z + u_1 \lambda)^2 + \varepsilon_1^2 u_1^2 \right] + Q_1 \theta_1 = 0 \quad (7)$$

$$\frac{d^2 B_{x1}}{dy^2} + \lambda Rm_1 \frac{du_1}{dy} = 0 \quad (8)$$

$$-mh^2 P + \frac{d^2 \hat{u}_2}{dy^2} + rbh^2 m \frac{Gr}{Re} \hat{\theta}_2 \sin \phi - Ha_2^2 \lambda (E_z + \hat{u}_2 \lambda) - \varepsilon_2^2 \hat{u}_2 = 0 ; \quad \text{where, } \varepsilon_2^2 = k_p h^2 \varepsilon_1^2 \quad (9)$$

$$\frac{d^2 \hat{\theta}_2}{dy^2} + Ec Pr \frac{k_c}{m} \left[ \left( \frac{d\hat{u}_2}{dy} \right)^2 + Ha_2^2 (E_z + \hat{u}_2 \lambda)^2 + \varepsilon_2^2 \hat{u}_2^2 \right] + Q_2 \hat{\theta}_2 = 0 ; \quad \text{where, } Ha_2^2 = smh^2 Ha_1^2 \quad (10)$$

$$\frac{d^2 \hat{B}_{x2}}{dy^2} - \lambda shm_e Rm_1 \frac{d\hat{u}_2}{dy} = 0 \quad (11)$$

The boundary conditions for the new domain  $[0,1]$  now become:

$$\left. \begin{array}{l} u_1(0) = \hat{u}_2(0) \\ \left. \frac{du_1}{dy} \right|_{y=0} = - \frac{1}{mh} \left. \frac{d\hat{u}_2}{dy} \right|_{y=0} \\ \theta_1(0) = \hat{\theta}_2(0) \\ \left. \frac{d\theta_1}{dy} \right|_{y=0} = - \frac{1}{k_c h} \left. \frac{d\hat{\theta}_2}{dy} \right|_{y=0} \\ B_{x1}(0) = \hat{B}_{x2}(0) \\ \left. \frac{dB_{x1}}{dy} \right|_{y=0} = - \frac{1}{shm_e} \left. \frac{d\hat{B}_{x2}}{dy} \right|_{y=0} \end{array} \right\} \text{ at } y=0 ; \quad \left. \begin{array}{l} u_1(1) = u_{w1} \\ \theta_1(1) = \theta_w \\ \hat{u}_2(1) = u_{w2} \\ \hat{\theta}_2(1) = 0 \\ B_{x1}(1) = 0 \\ \hat{B}_{x2}(1) = 0 \end{array} \right\} \text{ at } y=1 \quad (12.a-1)$$

### 3. SOLUTION METHODOLOGY

Due to presence of buoyancy force, Ohmic and viscous dissipations effects and porosity of the medium, the governing equations are coupled and non-linear, making difficult to find analytical solutions. In the present work, Eqs. (6) to (11), subjected to boundary conditions, Eqs. (12), are solved as a coupled system of first-order ordinary differential equations through a well-established numerical routine for solution of stiff two-point boundary value problems. The BVFPD routine (IMSL, 2006) solves a parameterized system of ordinary differential equations with boundary conditions at two or more points, using a variable order, variable step size finite difference method with deferred corrections. The resulting nonlinear algebraic system is solved by Newton's method with step control. The linearized system of equations is solved by a special form of Gauss elimination that preserves the sparseness. This routine, which provides an automatic control of the relative error, handles problems in the form:

$$\underline{\gamma}' = f[y, \underline{\gamma}(y)]^T, \quad y \in [a, b] \quad (13)$$

with boundary conditions:

$$g[\underline{\gamma}(a), \underline{\gamma}(b)] = 0 \quad (14)$$

To write the governing equations in this form, they must be firstly transformed to a system of first order differential equations. The following correspondence between vector  $\underline{\gamma}$  and the governing variables is firstly established.

$$\begin{aligned}\underline{\gamma} &= [\gamma_1, \gamma_2, \gamma_3, \gamma_4, \gamma_5, \gamma_6, \gamma_7, \gamma_8, \gamma_9, \gamma_{10}, \gamma_{11}, \gamma_{12}]^T \\ &= \left[ u_1, \frac{du_1}{dy}, \theta_1, \frac{d\theta_1}{dy}, \hat{u}_2, \frac{d\hat{u}_2}{dy}, \hat{\theta}_2, \frac{d\hat{\theta}_2}{dy}, B_{x1}, \frac{dB_{x1}}{dy}, \hat{B}_{x2}, \frac{d\hat{B}_{x2}}{dy} \right]^T\end{aligned}\quad (15)$$

Then, the original system of six second-order differential equations is transformed to a system of twelve first-order differential equations (vector,  $\underline{\gamma}$ ), as:

$$\frac{d\gamma_1}{dy} = \gamma_2 \quad (16.a)$$

$$\frac{d\gamma_2}{dy} = P - \frac{Gr}{Re} \gamma_3 \sin \phi + Ha_1^2 \lambda (E_z + \gamma_1 \lambda) + \varepsilon_1^2 \gamma_1 \quad (16.b)$$

$$\frac{d\gamma_3}{dy} = \gamma_4 \quad (16.c)$$

$$\frac{d\gamma_4}{dy} = -Ec Pr \left[ \gamma_2^2 + Ha_1^2 (E_z + \gamma_1 \lambda)^2 - \varepsilon_1^2 \gamma_1^2 \right] + Q_1 \gamma_3 \quad (16.d)$$

$$\frac{d\gamma_5}{dy} = \gamma_6 \quad (16.e)$$

$$\frac{d\gamma_6}{dy} = mh^2 P - bmrh^2 \frac{Gr}{Re} \gamma_7 \sin \phi + Ha_2^2 \lambda (E_z + \gamma_5 \lambda) + \varepsilon_2^2 \gamma_5 \quad (16.f)$$

$$\frac{d\gamma_7}{dy} = \gamma_8 \quad (16.g)$$

$$\frac{d\gamma_8}{dy} = -Ec Pr \frac{k_c}{m} \left[ \gamma_6^2 + Ha_2^2 (E_z + \gamma_5 \lambda)^2 + \varepsilon_2^2 \gamma_5^2 \right] + Q_2 \gamma_7 \quad (16.h)$$

$$\frac{d\gamma_9}{dy} = \gamma_{10} \quad (16.i)$$

$$\frac{d\gamma_{10}}{dy} = -\lambda Rm_1 \gamma_2 \quad (16.j)$$

$$\frac{d\gamma_{11}}{dy} = \gamma_{12} \quad (16.k)$$

$$\frac{d\gamma_{12}}{dy} = \lambda shm_e Rm_1 \gamma_6 \quad (16.l)$$

Subjected to left ( $y = 0$ ) and right ( $y = 1$ ) boundary conditions given by:

$$\left. \begin{aligned}\gamma_1(0) - \gamma_5(0) &= 0 \\ \gamma_2(0) + \frac{1}{mh} \gamma_6(0) &= 0 \\ \gamma_3(0) - \gamma_7(0) &= 0 \\ \gamma_4(0) + \frac{1}{k_c h} \gamma_8(0) &= 0 \\ \gamma_9(0) - \gamma_{11}(0) &= 0 \\ \gamma_{10}(0) + \frac{1}{shm_e} \gamma_{12}(0) &= 0\end{aligned} \right\}, \text{ at } y=0;$$

$$\left. \begin{aligned}\gamma_1(1) - u_{w1} &= 0 \\ \gamma_3(1) - \theta_w &= 0 \\ \gamma_5(1) - u_{w2} &= 0 \\ \gamma_7(1) &= 0 \\ \gamma_9(1) &= 0 \\ \gamma_{11}(1) &= 0\end{aligned} \right\}, \text{ at } y=1 \quad (17.a-1)$$

#### 4. RESULTS AND DISCUSSION

Numerical results are presented, illustrating the behavior of flow, magnetic and heat transfer fields for various values of the governing dimensionless parameters. The resulting first order system, Eqs. (16,17), was numerically implemented in a Fortran 90 language code and solved by routine BVFPD for a relative error target of  $10^{-10}$ , i.e., ten digits is the requirement for convergence of all twelve potentials in any transversal coordinate,  $y$ . These coordinates, initially set as a uniform mesh, are automatically changed by the routine, according to the problem requirements, to make the local error approximately the same size everywhere.

Results obtained with the present numerical approach are compared with some selected previous analytical and approximate numerical results aimed at to show the versatility of the present approach in handling different physical possibilities. Twenty four dimensionless parameters must be informed as input, namely:  $P$ ,  $Gr$ ,  $Re$ ,  $E_z$ ,  $\phi$ ,  $Ha_1$ ,  $\varepsilon_1$ ,  $Ec$ ,  $Pr$ ,  $m$ ,  $h$ ,  $r$ ,  $b$ ,  $s$ ,  $k_c$ ,  $k_p$ ,  $Q_1$ ,  $Q_2$ ,  $u_{w1}$ ,  $u_{w2}$ ,  $\theta_w$ ,  $\lambda$ ,  $m_e$  and  $Rm_1$ . Two additional parameters,  $Ha_2$  and  $\varepsilon_2$ , are obtained as function of the previous ones according to Eqs. (9) and (10), or set to a value for situations where  $Ha_1 = 0$  and/or  $\varepsilon_1 = 0$ .

Figures 2 and 3 bring comparisons with the analytical results of Malashetty and Leela (1992) for the forced convection of two immiscible and electric conducting fluids inside a horizontal channel with fixed plates. The following set of parameters were employed:  $P = -2$ ;  $Gr = 0$ ;  $Re = 1$ ;  $E_z = -1$ ;  $\phi = 0$ ;  $Ha_1 = 2, 10, 20$ ;  $\varepsilon_1 = 0$ ;  $Ec = 1$ ;  $Pr = 1$ ;  $m = 0.333$ ;  $h = 0.1$ ;  $r = 0$ ;  $b = 0$ ;  $s = 0.1, 2, 3$  ( $Ha_2 = 0.1632, 0.8161, 1.6322$ );  $k_c = 1$ ;  $k_p = 0$  ( $\varepsilon_2 = 0$ );  $Q_1 = Q_2 = 0$ ;  $u_{w1} = u_{w2} = 0$ ;  $\theta_w = 0$ ;  $\lambda = 1$ ;  $m_e = 1$ ;  $Rm_1 = 0$ . Malashetty and Leela (1992) used different scales to make temperature dimensionless, so that their dimensionless temperature fields are related to the present ones through  $\theta_i^* = \theta_i / (Ec Pr)$ .

Figures 2.a and 2.b show the behavior of velocity and temperature fields, respectively, as Hartmann number,  $Ha_1$ , is increased from 2 to 20 through 10, for electrical conductivity ratio,  $s$ , is fixed to 2. Figures 3.a and 3.b show the behavior of velocity and temperature fields, respectively, as ratio of electrical conductivity is increased from 0.1 to 3, for Hartmann number,  $Ha_1 = 10$ .

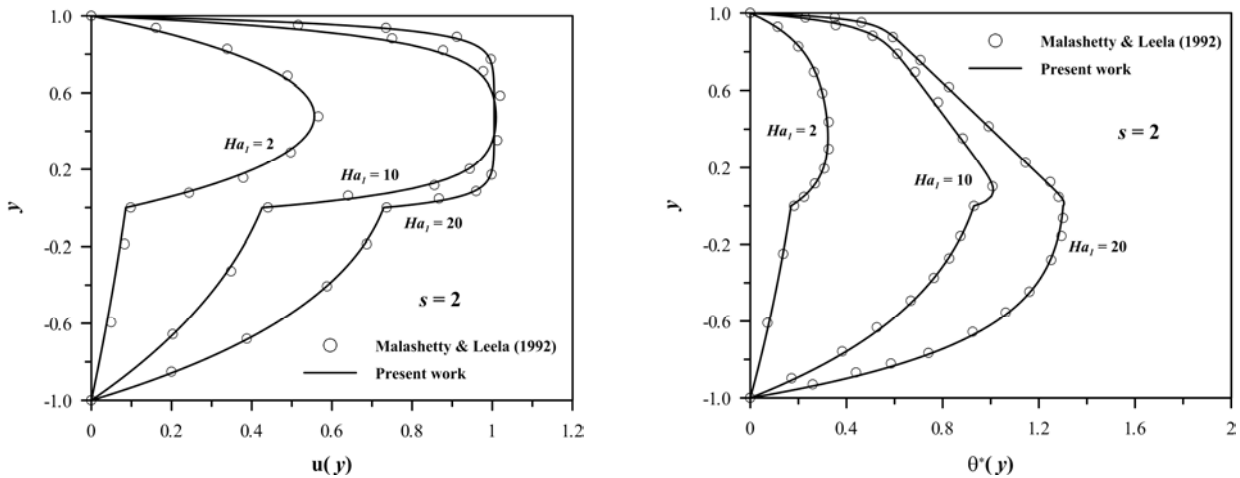


Figure 2. Profiles of (a) velocity and (b) temperature fields, for different Hartmann numbers.

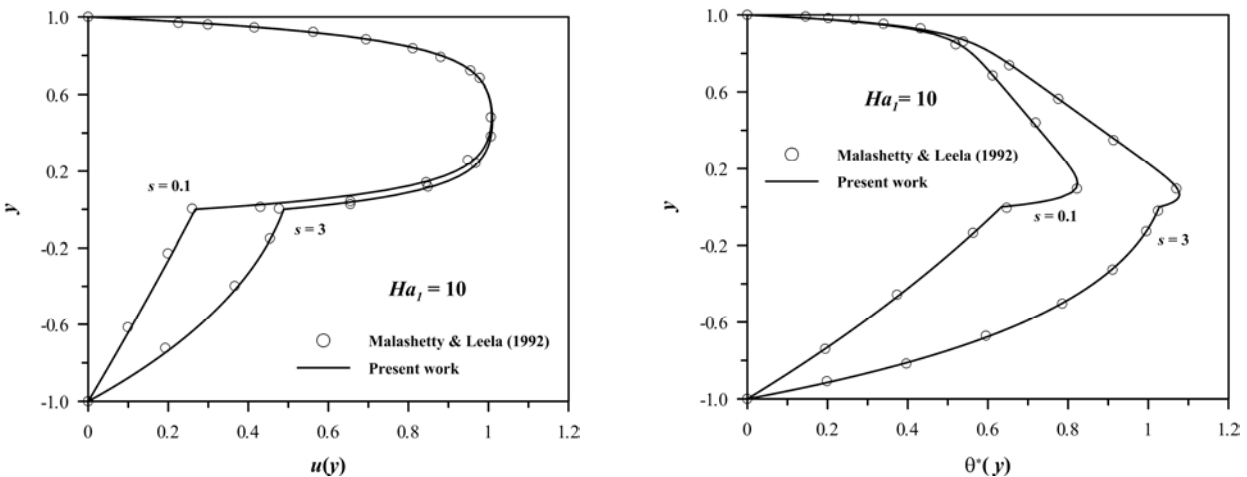


Figure 3. Profiles of (a) velocity and (b) temperature fields, for different electrical conductivity ratios.

As verified by Malashetty and Leela (1992), since the electrical load parameter is negative,  $E_z = -1$  (open circuited), the effect of the Lorentz force is to accelerate the flow (an electromagnetic pump) and increase the temperature inside the channel, in clear contrast with the short circuit case, where the electromagnetic force retards the flow and decreases the heat transfer. In turn, the effect of varying the electrical conductivity ratio,  $s$ , is more pronounced in the temperature field than in the velocity field, especially in region II. By increasing the electrical conductivity ratio, the temperature is also increased, because more energy is added by Joule heating.

Figures 4 bring comparisons with the approximate results of Malashetty *et al.* (2001b), who employed the regular perturbation method to study the mixed convection of two immiscible and electric conducting fluids inside a inclined channel with stationary plates. The following dimensionless parameters were employed:  $P = -5$ ;  $Gr = 5$ ;  $Re = 5$ ;  $E_z = 0$ ;  $\phi = 0, 30, 45, 75$ ;  $Ha_1 = 2$ ;  $\varepsilon_1 = 0$ ;  $Ec = 10^{-5}$ ;  $Pr = 1$ ;  $m = 0.5$ ;  $h = 1$ ;  $r = 1.5$ ;  $b = 1$ ;  $s = 0.1, 0.33, 1, 2$  ( $Ha_2 \cong 0.45, 0.81, 1.41, 2$ );  $k_c = 1$ ;  $k_p = 0$  ( $\varepsilon_2 = 0$ );  $Q_1 = Q_2 = 0$ ;  $u_{w1} = u_{w2} = 0$ ;  $\theta_w = 1$ ;  $\lambda = 1$ ;  $m_e = 1$ ;  $Rm_1 = 0$ .

Figures 4.a and 4.b show the behavior of velocity field as function of the channel angle of inclination and electrical conductivity ratio, respectively. In the first figure, the electrical conductivity ratio is fixed to 2 and the angle of inclination is allowed to vary from  $0^\circ$  to  $75^\circ$  through  $30^\circ$  and  $45^\circ$ . In Figure 4.b, the angle of inclination is set to  $30^\circ$  while the electrical conductivity ratio varies from 0.1 to 2 through 0.33 and 1.

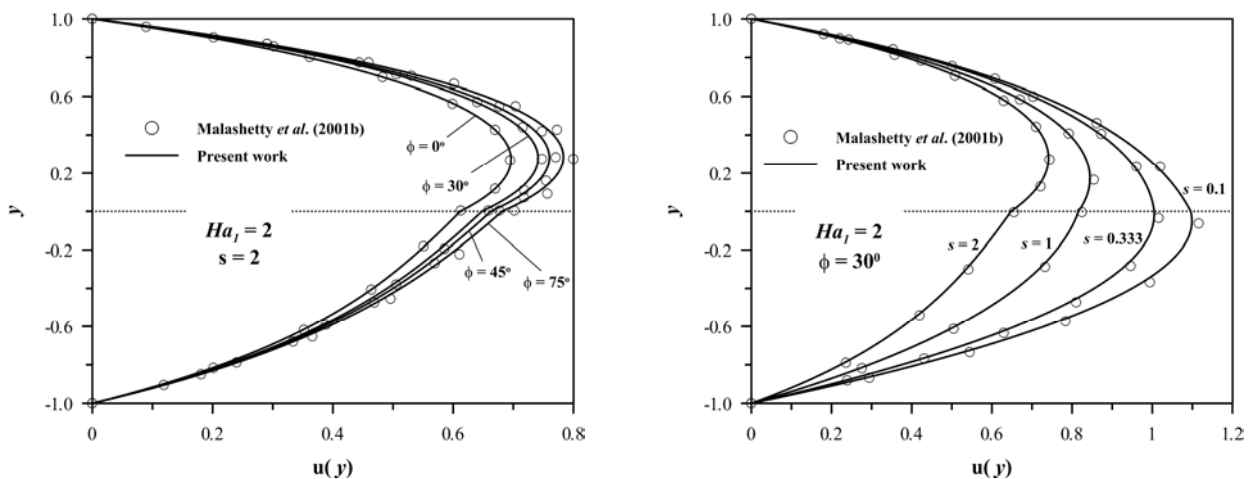


Figure 4. Velocity profiles for different (a) channel inclinations, and (b) electrical conductivity ratios.

Results are in good agreement with the approximate results of Malashetty *et al.* (2001b), except for the velocity profiles for large values of channel inclination, where a slight discrepancy is observed. This difference is possibly due to some error in the analytical expressions employed to generate the approximate solution, or introduced by the approximate method itself, even for small value of the product  $Ec.Pr$ .

Now, although the study on flow and heat transfer in porous channels does not directly relate to magnetohydrodynamics, the porous Brinkman terms in the momentum and energy equations in the former closely resemble the Lorentz force and the Joule dissipation effects in the latter. Thus, since the present formulation also allows for analysis of this kind of physics, comparisons with the results presented by Malashetty *et al.* (2004) are shown above. They studied the two-fluid flow and heat transfer in an inclined channel containing a porous top layer and a non-porous bottom layer through regular perturbation method, valid only for small values of a perturbation parameter, which in this case was chosen the product  $Ec.Pr$ .

Figures 5 illustrates the effects of the buoyancy force, channel inclination, and height and viscosity ratios on flow field behavior, for two values of medium porosity. The results were obtained using the following set of parameters:  $P = -5$ ;  $Gr = 5, 15, 25$ ;  $Re = 5$ ;  $E_z = 0$ ;  $\phi = 0, 30, 60, 90$ ;  $Ha_1 = 0$ ;  $\varepsilon_1 = 5, 20$ ;  $Ec = 10^{-5}$ ;  $Pr = 1$ ;  $m = 0.1, 1, 2$ ;  $h = 0.1, 1, 2$ ;  $r = 1.5$ ;  $b = 1$ ;  $s = 0$  ( $Ha_2 = 0$ );  $k_c = 1$ ;  $k_p = 0$  ( $\varepsilon_2 = 0$ );  $Q_1 = Q_2 = 0$ ;  $u_{w1} = u_{w2} = 0$ ;  $\theta_w = 1$ ;  $\lambda = 1$ ;  $m_e = 1$ ;  $Rm_1 = 0$ . For reproduction of the results presented in Figs. (5a-c), the viscosity ratio was set to  $m = 1$ , instead of  $m = 0.5$  as mistakenly described by Malashetty *et al.* (2004). This observation apart, the present results match the approximate results of Malashetty *et al.* (2004), although slightly differences are observed in Fig. (5c) in the non-porous layer, for large values of channel height ratio ( $h = 2$ ). If no other error is present in the analysis, this behavior is probably due to the inadequacy of the regular perturbation method when layer height ratio is increased.

Finally, as one can easily see, for the flow and temperature fields the effect of increasing the porosity parameter,  $\varepsilon_1$ , is the same as increasing the Hartmann number in a electrically conductor fluid, *i.e.*, to retard (and flat) the velocity profile and increase the heat generation. From the governing equations, the porosity parameter can be interpreted as an equivalent Hartmann number,  $\varepsilon_1^2 = (Ha_1 \lambda)^2$ .

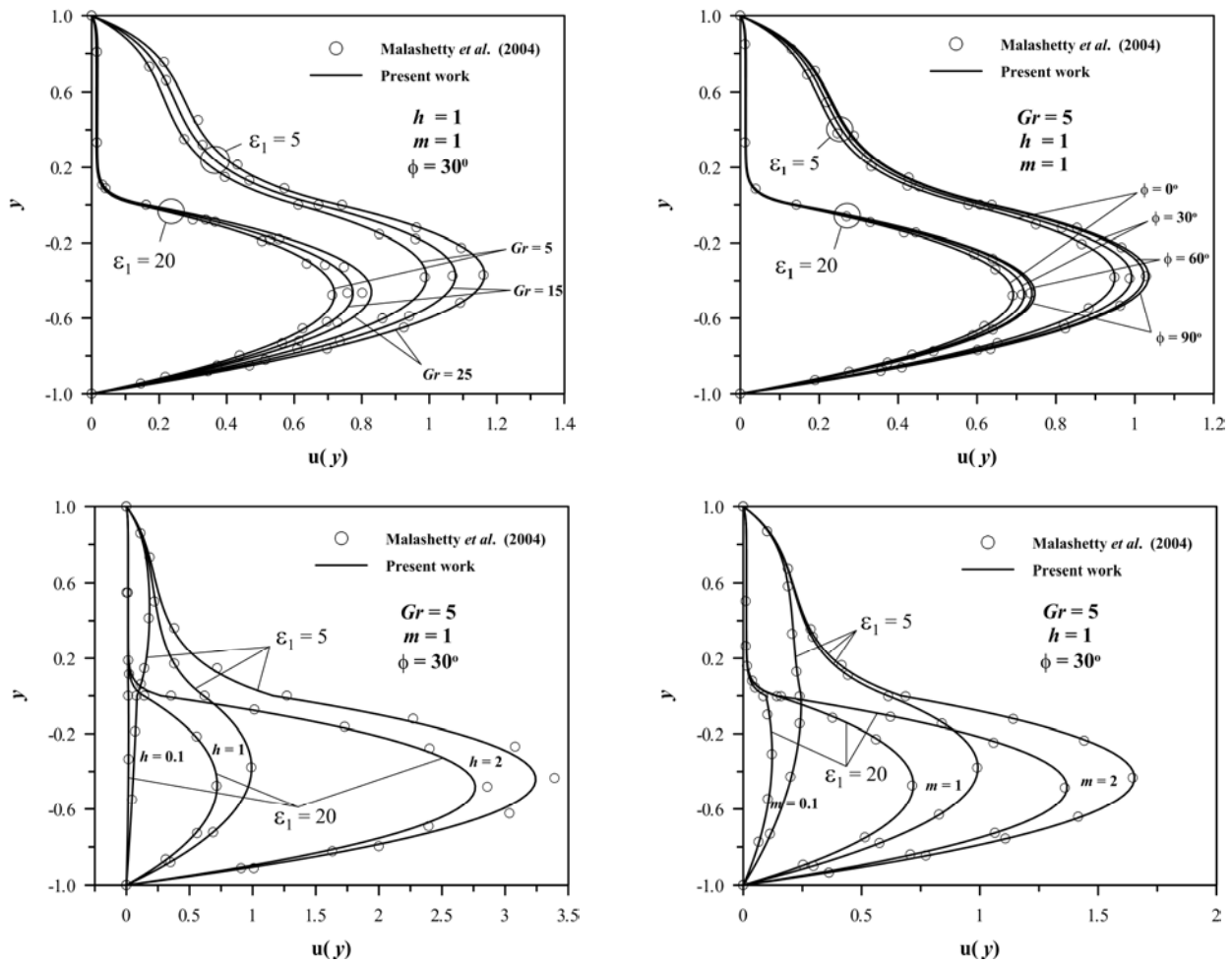


Figure 5. Velocity profiles for different top layer porosity and (a) Grashoff number, (b) channel inclination, (c) layer height ratio, and (d) fluid viscosity ratio.

Figures 6 and 7 illustrate comparisons with the results of Umavathi *et al.* (2005), who also employed the regular perturbation method, and the finite difference method for larger values of the product  $Ec.Pr$ , to study the mixed convection in a vertical channel of two immiscible and electric conducting fluids. In addition to Joule and viscous dissipation, heat source/sink possibilities are allowed to occur through appropriate choice of parameters  $Q_1$  and  $Q_2$ . The following set of parameters were employed:  $P = -5$ ;  $Gr = 5$ ;  $Re = 5$ ;  $E_z = -1, 0, 1$ ;  $\phi = 90^\circ$ ;  $Ha_1 = 4$ ;  $\epsilon_1 = 0$ ;  $Ec = 10^{-5}, 0.1, 0.5, 1$ ;  $Pr = 1$ ;  $m = 1$ ;  $h = 1$ ;  $r = 1$ ;  $b = 1$ ;  $s = 2$  ( $Ha_2 = 5.6569$ );  $k_c = 1$ ;  $k_p = 0$  ( $\epsilon_2 = 0$ );  $Q_1 = Q_2 = -10, -5, -0.001, 0.001, 1, 2, 4$ ;  $u_{w1} = u_{w2} = 0$ ;  $\theta_w = 1$ ;  $\lambda = 1$ ;  $m_e = 1$ ;  $Rm_1 = 0$ .

Figures 6.a and 6.b show the behavior of velocity and temperature fields, respectively, as function of the electrical load factor,  $E_z$ , and Eckert number,  $Ec$ , for heat generation case ( $Q_1 = Q_2 = 1$ ) and  $Ha_1 = 4$ . Results are in agreement for both potentials, except for the pair of positive electrical load factor ( $E_z = 1$ ) and large Eckert number ( $Ec = 1$ ). For increasing Eckert number, instabilities in the numerical computation begin to occur at approximately 0.815 and the ODE system seems to become extremely stiff or singular, although the numerical results presented by Umavathi *et al.* (2005) do not show this behavior. For values Eckert larger then 0.82, stability of the numerical computational is recovered, but flow and heat transfer behaviors are significantly modified relative to low Eckert numbers. In order to verify this discrepancy, other numerical platform was employed for this specific set of parameters. The same instability behavior was also verified, so it is here believed that the results presented by Umavathi *et al.* (2005) are probably not correct for  $Ec = 1$ .

Figures 7.a and 7.b illustrate the behavior of velocity field for heat generation ( $Q_1 = Q_2 = 0.001, 2, 4$ ) and absorption ( $Q_1 = Q_2 = -0.001, -5, -10$ ) situations, respectively, as function of the electrical load factor,  $E_z$ . Results were computed for  $Ha_1 = 4$ , for the heat generation case, and  $Ha_1 = 1$ , for the heat absorption one, maintaining  $Ec = 0.1$  in both situations. As it would be expected, flow behavior is markedly altered by the choice of heat source/sink parameter. For the heat generation situation, it is interesting to note that an increase in the heat generation parameter from 0.001 to 2 increases the velocity field, while an increase from 2 to 4 leads to an opposite effect. Although not shown, this behavior is also present in the temperature field.



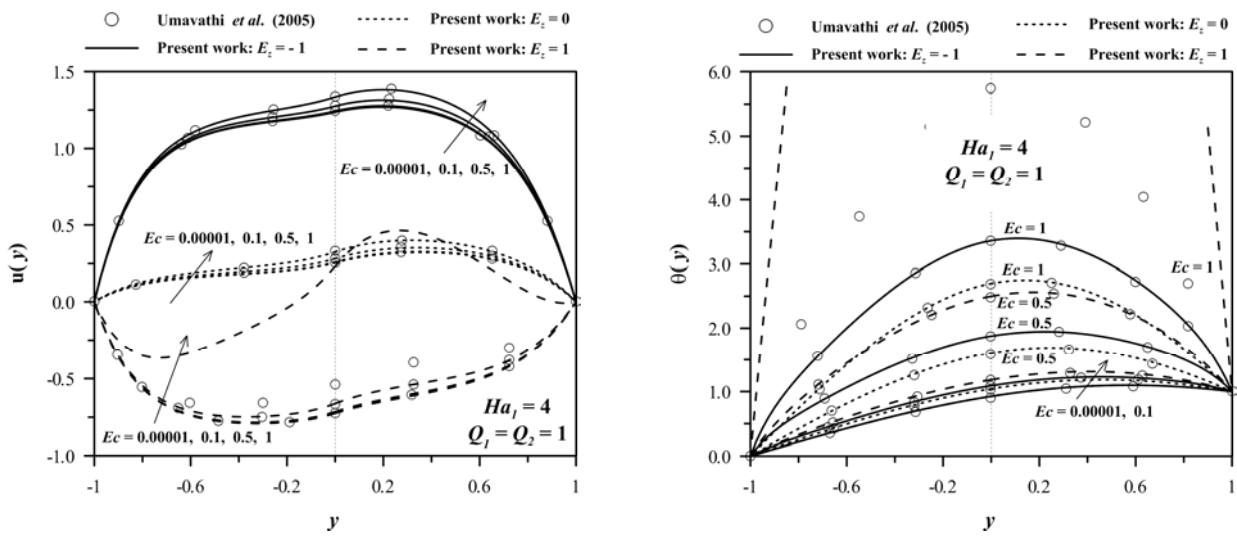


Figure 6. Profiles of (a) velocity and (b) temperature fields, for different pairs of Eckert number, and electrical load factor. Heat generation case.

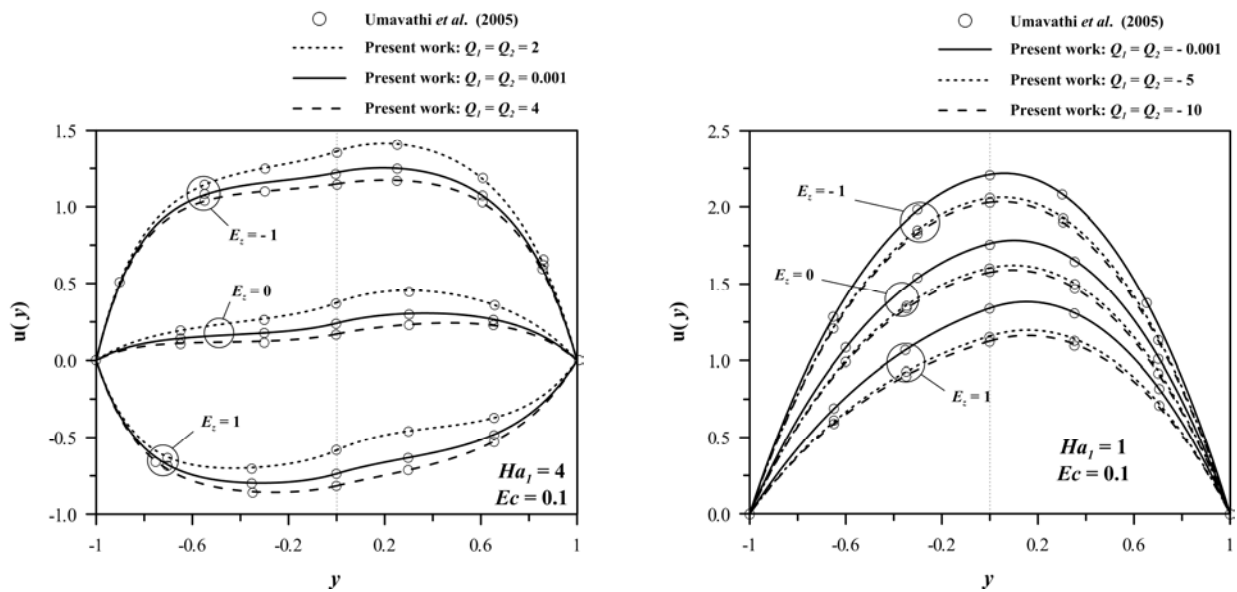


Figure 7. Velocity profiles for different electrical load factors,  $E_z$ . (a) heat generation and (b) heat absorption.

Attention is now directed to the influence of moving plates on flow and heat transfer characteristics of two-phase immiscible magnetohydrodynamic fluid flow. Mixed convection in an inclined channel with the top plate moving with constant velocity was studied by Umavathi et al. (2010) through regular perturbation method. Only the fluid on the bottom side of the channel was electrically conductor. By its turn, Zivojin et al. (2010) studied, analytically, the forced convection of two-immiscible electrically conductor fluids in a horizontal channel where both plates are allowed to move with constant velocity and opposite directions. Since they considered inclined magnetic field relative to the transversal  $y$  axis, the induced magnetic field on flow direction,  $x$ , was also evaluated.

Figures 8 bring comparisons between the present results for the velocity and temperature fields with the results of Umavathi et al. (2010), illustrating the influence of Grashof number (Fig. 8.a), channel inclination (Fig. 8.b) and thermal conductivity ratio (Fig. 8.c) on flow field, and of thermal conductivity ratio on the temperature field. The following dimensionless set was employed:  $P = -5$ ;  $Gr = 5, 10, 15, 20$ ;  $Re = 1$ ;  $E_z = 0$ ;  $\phi = 0, 30, 45, 90^\circ$ ;  $Ha_1 = 0$ ;  $\epsilon_1 = 0$ ;  $Ec = 0.01$ ;  $Pr = 0.7$ ;  $m = 1$ ;  $h = 1$ ;  $r = 1$ ;  $b = 1$ ;  $Ha_2 = 2$ ;  $k_c = 0.667, 1, 2, 10$ ;  $k_p = 0$  ( $\epsilon_2 = 0$ );  $Q_1 = Q_2 = 0$ ;  $u_{w1} = 1$ ;  $u_{w2} = 0$ ;  $\theta_w = 1$ ;  $\lambda = 1$ ;  $m_e = 1$ ;  $Rm_1 = 0$ . Note that, since only the fluid in Region II is electrically conductor,  $Ha_1 = 0$ , and  $Ha_2$  is set to a specific value (in the present work,  $Ha_2 = 2$ ), regardless the value used for the electrical conductivity ratio,  $s$ .

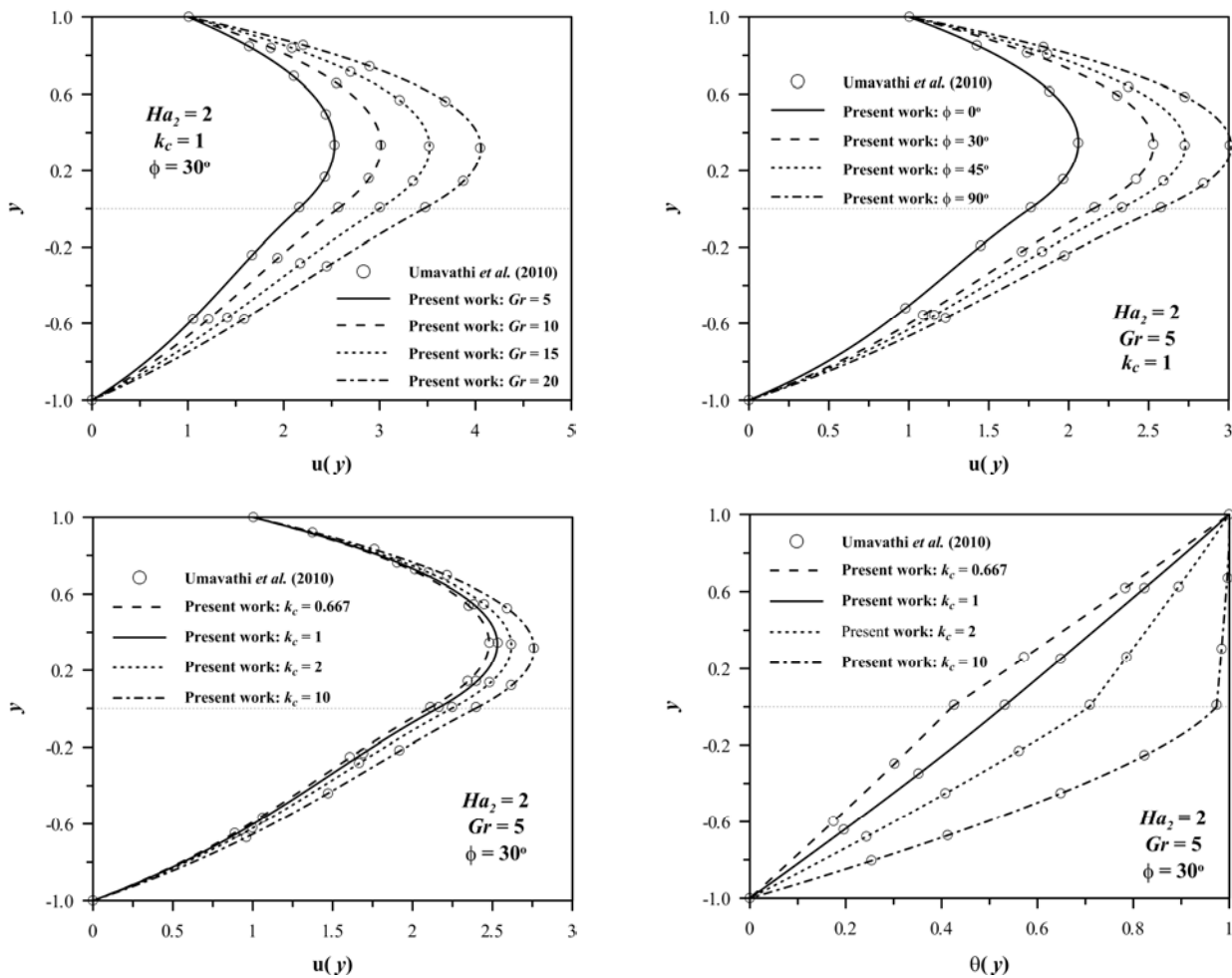


Figure 8. Velocity profiles as function of (a) Grashof number, (b) channel inclination, and (c) thermal conductivity ratio. (d) Temperature profile as function of the thermal conductivity ratio.

The expected behavior of the velocity field with Grashof number and channel inclination is naturally predicted by the present approach, the results of which match those obtained by Umavathi *et al.* (2010) through the regular perturbation approximate method. As the Grashof number and the inclination angle increase there is an enhancement of flow and heat transfer rates inside the channel, since the buoyancy forces are proportional to these parameters. These results confirm the possible mistakes observed on the results of Malashetty *et al.* (2001b), Fig. 4a. Additionally, an increase in the thermal conductivity ratio increases the velocity and, more markedly, the temperature field.

Figures 9.a and 9.b bring comparisons for the velocity and temperature fields with the results of Zivojin *et al.* (2010), illustrating the influence of the inclination of the magnetic field on these potentials. Figures 10.a and 10.b show the influence of the inclination of the magnetic field and the Hartmann number on the induced magnetic field, respectively. In order to make the comparisons, the following dimensionless groups were employed:  $P = -3.5$ ;  $Gr = 0$ ;  $Re = 1$ ;  $E_z = -1, 0, 1$ ;  $\phi = 0$ ;  $Ha_1 = 1, 2, 3$ ;  $\varepsilon_l = 0$ ;  $Ec = 1$ ;  $Pr = 1$ ;  $m = 0.66$ ;  $h = 1$ ;  $r = 1$ ;  $b = 1$ ;  $s = 37.9$  ( $Ha_2 = 5, 10, 15$ );  $k_c = 0.06$ ;  $k_p = 0$  ( $\varepsilon_2 = 0$ );  $Q_1 = Q_2 = 0$ ;  $u_{w1} = 1$ ;  $u_{w2} = -1$ ;  $\theta_w = 1$ ;  $\lambda = 0.5, 0.75, 1$ ;  $m_e = 1$ ;  $Rm_l = 0.8 \times 10^{-9}$ . Zivojin *et al.* (2010) used different scales to make the temperature fields dimensionless, so their dimensionless temperature fields are related to the present ones through  $\theta_1^* = (\theta_1 - 1)/(Ec Pr)$  and  $\theta_2^* = \theta_2 m/(k_c Ec Pr)$ .

The present results match the analytical solutions obtained by Zivojin *et al.* (2010) for all potentials analyzed. Here, it is worth to verify the effect of the opposite top and bottom plates velocities on flow behavior. Figure 9.a shows that the point where velocity is zero is displaced from the channel center, because the viscosity ratio,  $m$ , is different from unity, regardless the inclination of the external magnetic field. By its turns, Figure 9.b shows a jump in the temperature at the interface ( $y = 0$ ), which, as explained by Zivojin *et al.* (2010), results from their choice of the dimensionless groups for the temperature fields.

As for velocity and temperature fields, results obtained for the induced magnetic field (Fig. 10.a and 10.b) match the analytical solutions, and illustrate the strong influence of the inclination angle of the external magnetic field and the Hartmann number on this potential. Since fluid in Region II is more electrically conductive ( $s = \sigma_2/\sigma_1 = 37.9$ ), effect of Hartmann number is more pronounced in this region.

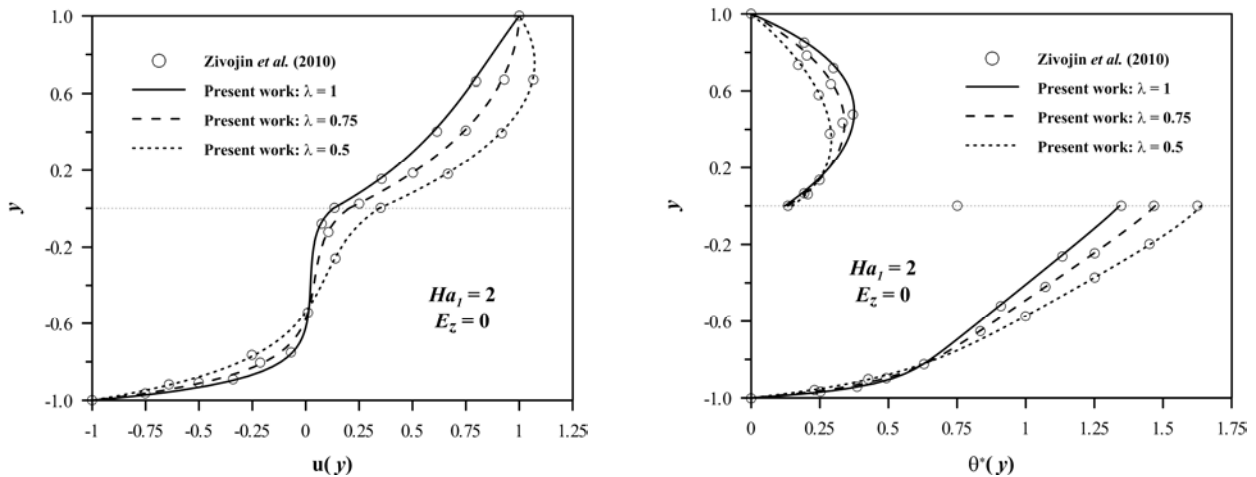


Figure 9. Profiles for (a) velocity, and (b) temperature fields for different external magnetic field inclinations.

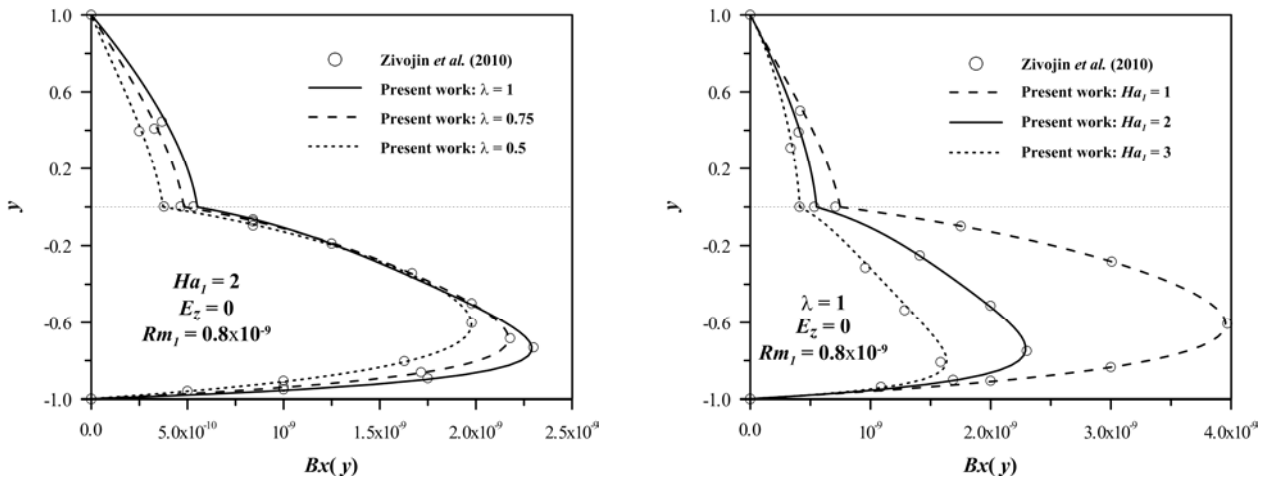


Figure 10. Induced magnetic field for different (a) external magnetic field inclination, and (b) Hartmann number.

Here, it is important to mention that, although the magnetic Reynolds number,  $Rm_1$ , is small (a hypothesis adopted in order to not take into account any disturbance of the external magnetic field), and so is the induced magnetic field,  $Bx$ , the general conclusions obtained under this hypothesis are also valid for higher values of the magnetic Reynolds number. Therefore, the study of these simpler situations can bring some basic knowhow for analysis of more complicated physics.

## 5. CONCLUSIONS

The results obtained, validated against analytical solutions and compared with other approximate numerical methods, clearly show the simplicity, efficiency and robustness of the present approach for analysis of a broad spectrum of problems governed by two-point boundary value ordinary differential equations, here in particular, those related to magnetohydrodynamic of two-immiscible flow. As demonstrated in the results section, several physical situations (with greater emphasis on magnetohydrodynamics) have been handled through this single procedure. Its main applicability lies, of course, on problem where no analytical solutions is possible, or difficult to be found. Additionally, since hybrid methods, such as the Generalized Integral Transform Technique (GITT), employ intensively routines for initial and boundary value problems (like BVPFD and IVPAG, IMSL (2006)) to solve the resulting transformed ODE systems, the present work serves as a physical and mathematical starting point for application of such techniques on developing two-phase heat and fluid MHD flow inside channels (Lima and Rêgo, 2013). Therefore, the main goals of the present work were successfully reached, namely, to develop a basic background on magnetoconvection inside channels, and present part of the numerical approach employed by GITT to solve boundary value problems with emphasis on two-phase magnetohydrodynamics flow with heat transfer. Currently, hybrid analyses on developing two-phase flow with heat transfer within channels are being performed by the present research group.

## 6. REFERENCES

- Alpher, R.A., 1961. "Heat transfer in magnetohydrodynamic flow between parallel plates". *International Journal of Heat and Mass Transfer*, Vol. 3, pp. 108-112.
- Attia, H.A. and Kotb, N.A., 1996. "MHD flow between two parallel plates with heat transfer". *Acta Mechanica*, Vol. 117, pp. 215-220.
- Attia, H.A., 1998. "Hall current effects on the velocity and temperature fields of an unsteady Hartmann flow". *Canadian Journal of Physics*, Vol. 76, pp. 739-746.
- Attia, H.A., 1999. "Transient MHD flow and heat transfer between two parallel plates with temperature dependent viscosity". *Mechanics Research Communications*, Vol. 26, issue 1, pp. 115-121.
- Attia, H.A., 2006. "Steady MHD Couette flow with temperature-dependent physical properties". *Archives of Applied Mechanics*, Vol. 75, pp. 268-278.
- Attia H.A. and Aboul-Hassan, A.L., 2003. "The effect of variable properties on the unsteady Hartmann flow with heat transfer considering the Hall effect". *Applied Mathematical Modelling*, Vol. 27, pp. 551-563.
- Davidson, P.A., 2001. *An Introduction to Magnetohydrodynamics*. Cambridge University Press, Cambridge, UK.
- IMSL, 2006. IMSL Fortran Numerical Libraries, Version 6.0, Visual Numerics Inc.
- Klemp, K., Herwig, H. and Selmann, M., 1990. "Entrance flow in channel with temperature dependent viscosity including viscous dissipation effects". In *Proceedings of the 3rd International Congress of Fluid Mechanics*, Cairo, Egypt, Vol. 3, pp. 1257-1266.
- Lima, J.A. and Rêgo, M.G.O., 2013. "On the integral transform solution of low-magnetic MHD flow and heat transfer in the entrance region of a channel. *International Journal of Non-Linear Mechanics*, vol. 50, pp. 25-39.
- Lohrasbi, J. and Sahai, V., 1988. "Magnetohydrodynamic heat transfer in two phase flow between parallel plates". *Applied Scientific Research*, Vol. 45, pp. 53-66.
- Malashetty, M.S. and Leela, V., 1991. "Magnetohydrodynamic heat transfer in two fluid flow". In *Proceedings of the ASME/AIChE 27th National Heat Transfer Conference and Exposition*, **onde**, pp.28-31.
- Malashetty, M.S. and Leela, V., 1992. "Magnetohydrodynamic heat transfer in two phase flow". *International Journal of Engineering Science*, Vol. 30, Issue 3, pp. 371-377.
- Malashetty, M.S. and Umavathi, J.C., 1997. "Two-phase magnetohydrodynamic flow and heat transfer in an inclined channel". *International Journal of Multiphase Flow*, Vol. 22, Issue 3, pp. 545-560.
- Malashetty, M.S., Umavathi, J.C. and Prathap Kumar, J., 2001a. "Two-fluid magnetoconvection flow in an inclined channel". *International Journal of Transport Phenomena*, Vol. 3, Issue 2, pp. 1-12.
- Malashetty, M.S., Umavathi, J.C. and Prathap Kumar, J., 2001b. "Convective magnetohydrodynamic two fluid flow and heat transfer in an inclined channel". *Heat and Mass Transfer*, Vol. 37, pp. 259-264.
- Malashetty, M.S., Umavathi J.C. and Prathap Kumar, J., 2004. "Two fluid flow and heat transfer in an inclined channel containing porous and fluid layer". *Heat and Mass Transfer*, Vol. 40, pp. 871-876.
- Malashetty, M.S., Umavathi, J.C. and Prathap Kumar, J., 2006. "Magnetoconvection of two-immiscible fluids in vertical enclosure". *Heat and Mass Transfer*, Vol. 42, pp. 977-993.
- Nigam, S.D. and Singh, S.N., 1960. "Heat transfer by laminar flow between parallel plates under the action of transverse magnetic field". *Quarterly Journal of Mechanics and Applied Mathematics*, Vol. 13, pp. 85-97.
- Nikodijevic, D., Milenkovic, D and Stamenkovic, Z., 2011. "MHD Couette two-fluid flow and heat transfer in presence of uniform inclined magnetic field". *Heat and Mass Transfer*, Vol. 47, pp. 1525-1535.
- Perlmutter, M. and Siegel, R., 1961. "Heat transfer to an electrically conducting fluid flowing in a channel with transverse magnetic field". NACA TN D-875.
- Roming, M. F., 1961. "The influence of electric and magnetic fields on heat transfer to electrically conducting fluids". *Advances in Heat Transfer*, Vol. 1, New York, Academic Press.
- Setayesh, A. and Sahai, V., 1990. "Heat transfer in developing magnetohydrodynamic Poiseuille flow and variable transport properties". *International Journal of Heat and Mass Transfer*, Vol. 33, Issue 8, pp. 1711-1720.
- Shail, R., 1973. "On laminar two-phase flows in magnetohydrodynamics". *International Journal of Engineering Science*, Vol. 11, pp. 1103-1108.
- Tao, L.N., 1960. "Magnetohydrodynamic effects on the formation of Couette flow". *Journal of the Aerospace Sciences*, Vol. 27, pp. 334-338.
- Umavathi, J.C., Chamka, Ali J., Manjula, M.H. and Ali Al-Mudhai, 2005. "Magneto-convection of a two-fluid flow through a vertical channel". *Heat and Technology*, Vol. 23, Issue, 2, pp. 151-163.
- Umavathi, J.C., Liu, I-C. and Prathap Kumar, J., 2010. "Magnetohydrodynamic Poiseuille-Couette flow and heat transfer in an inclined channel". *Journal of Mechanics*, Vol. 26, Issue 4, 525-532.
- Van Gorder, R., Prasad, K.V. and Vajravelu, K., 2012. "Convective heat transfer in the vertical channel flow of a clear fluid adjacent to a nanofluid layer: a two-fluid model". *Heat and Mass Transfer*, Vol. 48, pp. 1247-1255.
- Zivojin, S.M., Nikodijevic, D.D., Blagojevic, B.D. and Savic, S.R., 2010. "MHD flow and heat transfer of two immiscible fluids between moving plates". *Transactions of the Canadian Society for Mechanical Engineering*, Vol. 23, Issues 3-4, pp. 351-372.